Fat Distribution Patterns and Future Type 2 Diabetes

Hajime Yamazaki,[1] Shinichi Tauchi,[2] Jürgen Machann,[3,4,5] Tobias Haueise,[3,4,5] Yosuke Yamamoto,[6] Mitsuru Dohke,[7] Nagisa Hanawa,[7] Yoshihisa Kodama,[8] Akio Katanuma,[9] Norbert Stefan,[4,5,10] Andreas Fritsche,[4,5,10] Andreas L. Birkenfeld,[4,5,10] Róbert Wagner,[4,5,10,11,12] and Martin Heni[4,5,10,13,14]

Diabetes 2022;71:1937–1945 | https://doi.org/10.2337/db22-0315

Fat accumulation in the liver, pancreas, skeletal muscle, and visceral bed relates to type 2 diabetes (T2D). However, the distribution of fat among these compartments is heterogenous and whether specific distribution patterns indicate high T2D risk is unclear. We therefore investigated fat distribution patterns and their link to future T2D. From 2,168 individuals without diabetes who underwent computed tomography in Japan, this case-cohort study included 658 randomly selected individuals and 146 incident cases of T2D over 6 years of follow-up. Using data-driven analysis (k-means) based on fat content in the liver, pancreas, muscle, and visceral bed, we identified four fat distribution clusters: hepatic steatosis, pancreatic steatosis, trunk myosteatosis, and steatopenia. In comparisons with the steatopenia cluster, the adjusted hazard ratios for incident T2D were 4.02 (95% CI 2.27–7.12) for the hepatic steatosis cluster, 3.38 (1.65–6.91) for the pancreatic steatosis cluster, and 1.95 (1.07–3.54) for the trunk myosteatosis cluster. The clusters were replicated in 319 German individuals without diabetes who underwent MRI and metabolic phenotyping. The distribution of the glucose area under the curve across the four clusters found in Germany was similar to the distribution of T2D risk across the four clusters in Japan. Insulin sensitivity and insulin secretion differed across the four clusters. Thus, we identified patterns of fat distribution with different T2D risks presumably due to differences in insulin sensitivity and insulin secretion.

The incidence of type 2 diabetes (T2D) is increasing, and more individualized approaches to preventing and treating T2D are needed (1). Obesity is the main modifiable risk factor for T2D. The classification of obesity is typically based on BMI. Although BMI is an easy-to-determine indicator of overall adiposity, it gives no information about the location of accumulated fat. This is important, as the location of fat storage appears to be crucial for T2D risk (2).

Fat accumulation in the visceral bed (2,3), liver (4–6), pancreas (7,8), and skeletal muscle (9,10) is associated with T2D. "Visceral fat" refers to accumulation of adipose tissue in the peritoneum and retroperitoneum (11). Having large amounts of visceral fat is strongly linked to whole-body insulin resistance, which is an important predictor of T2D risk (3,11). Further important locations for excessive lipid accumulation include the liver (in hepatocytes), pancreas (in adipocytes), and skeletal muscle (intramyocellular

[1]Section of Clinical Epidemiology, Department of Community Medicine, Graduate School of Medicine, Kyoto University, Kyoto, Japan
[2]Department of Radiology, Keijinkai Maruyama Clinic, Sapporo, Japan
[3]Section on Experimental Radiology, Department of Radiology, Eberhard-Karls University, Tübingen, Germany
[4]German Center for Diabetes Research (DZD), Neuherberg, Germany
[5]Institute for Diabetes Research and Metabolic Diseases, Helmholtz Center Munich, University of Tübingen, Tübingen, Germany
[6]Department of Healthcare Epidemiology, School of Public Health, Graduate School of Medicine, Kyoto University, Kyoto, Japan
[7]Department of Health Checkup and Promotion, Keijinkai Maruyama Clinic, Sapporo, Japan
[8]Department of Radiology, Teine Keijinkai Hospital, Sapporo, Japan
[9]Center for Gastroenterology, Teine Keijinkai Hospital, Sapporo, Japan
[10]Division of Diabetology, Endocrinology and Nephrology, Department of Internal Medicine, Eberhard-Karls University, Tübingen, Germany
[11]German Diabetes Center (DDZ), Leibniz Center for Diabetes Research, Heinrich-Heine-University Düsseldorf, Düsseldorf, Germany
[12]Department of Endocrinology and Diabetology, University Hospital Düsseldorf, Heinrich-Heine-University Düsseldorf, Düsseldorf, Germany
[13]Department for Diagnostic Laboratory Medicine, Institute for Clinical Chemistry and Pathobiochemistry, University Hospital Tübingen, Tübingen, Germany
[14]Department of Internal Medicine I, University of Ulm, Ulm, Germany

Corresponding author: Hajime Yamazaki, yamazaki-myz@umin.ac.jp

Received 4 April 2022 and accepted 8 June 2022

This article contains supplementary material online at https://doi.org/10.2337/figshare.20060318.

R.W. and M.H. contributed equally.

and in adipocytes). Proposed mechanisms connecting increased lipid deposition in these three organs with T2D include hepatic insulin resistance (12,13), impairment of pancreatic insulin secretion (8,14), and muscle insulin resistance (9,15), respectively. The development of T2D probably depends on a complex interplay of those three mechanisms (13,14). Indeed, our previous longitudinal study showed how T2D risk is related to an interaction between obesity and pancreas fat (7), for which there is also histological and genetic evidence (16,17). While it has been proposed that some individuals have distinct patterns of body fat distribution that determine their likelihood to develop T2D (7,10,18), the approaches that led to those proposals were often hypothesis-driven and focused on effects of a limited number of fat compartments.

To identify previously undetected patterns of fat storage, we did a case-cohort study in Japan, using data-driven cluster analysis to partition participants based on the distribution of liver, pancreas, muscle, and visceral fat measured by computed tomography (CT). We then studied the longitudinal association of membership in the resulting clusters with incident T2D. Then, cluster validation was done in Germany among individuals with increased risk of T2D. In that study, body fat was quantified with MRI and ^{1}H-MRS and additional glycemic traits were assessed through 75-g oral glucose tolerance tests (OGTT).

RESEARCH DESIGN AND METHODS

We conducted a retrospective case-cohort study in Japan and a cross-sectional study in Germany. Case-cohort studies use data from individuals who are randomly selected members (i.e., subcohort) of a "total" cohort, and they additionally use data on all of the cases in which the outcome of interest occurred. This leads to efficient sampling by reducing the need to perform expensive measurements in a large sample of control subjects, while still using information on all cases, even if the outcome is not frequent (19). The benefit of the case-cohort design over a case-control design is that the randomly selected subcohort can be used to estimate characteristics of the total cohort and to select control subjects for multiple outcomes (20). A study flow diagram with an explanation of the methods can be found in Supplementary Fig. 1.

Participants in Japan

We used secondary data collected during health examinations with CT at Keijinkai Maruyama Clinic. CT equipment is easily accessible in Japan (21). We examined data from 2,793 individuals who underwent health examinations including baseline CT between 1 May 2008 and 31 March 2013. We excluded all individuals with diabetes at baseline (n = 216), as well as those who met CT exclusion criteria (n = 27), those whose BMI data were missing (n = 1), and those without follow-up data (n = 381). A radiologist, who was blinded to data other than CT images, excluded individuals with baseline CT scans that had substantial artifacts, as well as those with pancreatic calcification, space-occupying lesions in the pancreas, ambiguous pancreatic margin, pancreatic atrophy, splenic resection, or pancreatic resection. From the original 2,793 individuals, 2,168 were eligible for this study (i.e., the "total" cohort). During the median follow-up period of 6.27 years (interquartile range 4.04–8.20), there were 146 incident cases of T2D in the total cohort. From the viewpoint of relative efficiency (22), a 1:4 ratio of case:control subjects was favorable for this case-cohort study. We randomly selected 30% of the total cohort, and that 30% (658 participants) thus became the subcohort. After pooling this randomly selected subcohort and all remaining incident T2D case subjects who were not selected in this subcohort, we obtained a 1:4 ratio of case:noncase subjects (n = 146 and 608, respectively). There were 50 participants who had an incident case of T2D and were also in the randomly selected subcohort. Altogether, this case-cohort study comprised 754 participants.

Participants in Germany

We used secondary data from the Tübingen Diabetes Family Study (TDFS) (23), with recruitment of individuals with at least one of the following: known prediabetes, family history of diabetes, history of gestational diabetes mellitus, or obesity. We included individuals who underwent MRI/^{1}H-MRS to quantify visceral fat (T1-weighted fast spin echo), liver fat (^{1}H-MRS), pancreas fat, and muscle fat (three-dimensional multiecho chemical-shift encoding-based abdominal MRI), enabling assessment of all fat compartments corresponding to the CT study.

Measurement of Indices of Fat Distribution in Japan

We quantified four fat distribution indices on unenhanced CT: liver attenuation (liver fat), pancreas attenuation (pancreas fat), muscle attenuation (fat in trunk muscle), and visceral fat area (visceral fat). We also measured muscle area. Unenhanced CT images in which each slice was 10 mm thick were obtained with a single helical scanner (Asteion KG TSX-021B; Toshiba, Otawara, Japan) and a multislice helical scanner (Alexion TSX-032A; Toshiba) before and after May 2012, respectively.

Using a workstation (TWS-5000; Toshiba), and under the supervision of a radiologist, seven radiologic technologists who were blinded to data other than CT images measured liver attenuation and pancreas attenuation. Lower liver attenuation (Hounsfield units [HU]) indicated greater hepatic steatosis (24). Three round regions of interest (ROIs) with areas of 1.0 cm^2 were positioned on the hepatic anterior segment, posterior segment, and left lobe. The mean attenuation of those three ROIs was used to derive liver fat content. Our previous study regarding interrater reliability of this measure demonstrated an excellent intraclass correlation coefficient of 0.98 (95% CI 0.96–0.99) (7). Similarly, we measured pancreas fat by analyzing pancreas attenuation on CT images. This measure also negatively

correlates with pancreas fat (25). Three ROIs with areas of 1.0 cm^2 were positioned on thick segments of the pancreatic head, body, and tail to minimize partial-volume effects. The mean pancreas attenuation from these three ROIs was used as the index of pancreatic steatosis. Our previous study regarding interrater reliability showed an intraclass correlation coefficient of 0.89 (95% CI 0.82–0.94) (7).

Using an Automated Body composition Analyzer using Computed tomography image Segmentation (ABACS) software (Voronoi Health Analytics, Vancouver, Canada) and sliceOmatic software (TomoVision, Magog, Canada), an experienced radiologic technologist who was blinded to participants' information measured muscle area, muscle attenuation, and visceral fat area at the level of the L3 lumbar segment. Previous studies showed that L3-level measurements of muscle area and visceral fat area had the highest correlation with whole-body muscle and whole-body visceral fat (26). The ABACS software automatically recognizes these tissues based on CT attenuation thresholds (27). Muscle attenuation was automatically calculated as mean attenuation of muscle area. Lower muscle attenuation indicates more muscle fat (28,29). We evaluated intrarater reliability in 50 randomly selected participants: intraclass correlation coefficients of muscle area, muscle attenuation, and visceral fat area were all 1.00.

Measurement of Indices of Fat Distribution in Germany

All magnetic resonance (MR) examinations were performed with a 3T whole-body imager (MAGNETOM Vida; Siemens Healthineers, Erlangen, Germany). Visceral fat volume, pancreas fat, and muscle fat were measured with MRI, and liver fat was quantified with ^{1}H-MRS. Additionally, muscle area was measured. Volumetric quantification of visceral fat was performed from T1-weighted fast spin echo images with a slice thickness of 10 mm acquired between the hip and the thoracic diaphragm (30) with application of an automatic fuzzy c-means algorithm and orthonormal snakes (31). For determination of proton density fat fraction (PDFF) in pancreas and muscle, a three-dimensional multiecho gradient-echo chemical shift encoding-based technique was applied, with recording of six images with different echo times and a slice thickness of 3 mm in a single breath hold (32). Pancreas fat was quantified by manual drawing of three ROIs in the head, body, and tail of the pancreas. ^{1}H-MRS of the liver was done with application of a single-voxel STimulated Echo Acquisition Mode (STEAM) technique in a volume of interest of 3 × 3 × 2 cm^3 in the posterior part of segment VII (30). Signals of methylene and methyl protons (fat) were referenced to the sum of the fat and water signals to calculate liver fat in percent. All evaluations were performed by an experienced medical physicist on a standalone PC using MATLAB R2014A (MathWorks, Natick, MA) for visceral fat and liver fat measurement and on the workstation of the imager for pancreas fat measurement. Muscle fat and muscle area were assessed at the level of the L3 lumbar segment. For this purpose, a random sample of 50 manually segmented PDFF MR images at the level of the L3 lumbar segment were used to train an ensemble of five two-dimensional U-Net models (nnU-Net) (33) with fivefold cross validation to perform the segmentation of muscle PDFF on a cluster graphics processing unit (Tesla V100; NVIDIA, Santa Clara, CA). The nnU-Net ensemble showed a mean Dice similarity coefficient of 0.9725 (95% CI 0.9705–0.9744). The mean PDFF and MR image pixel dimensionality were used to derive the muscle fat and muscle area from the automatically segmented muscles, respectively (Supplementary Fig. 2).

Assessment of T2D Incidence in Japan

The presence of at least one of the following criteria was used to diagnose T2D: fasting plasma glucose ≥126 mg/dL, HbA1c ≥6.5% (48 mmol/mol), or having a prescription for any antidiabetes medication. The incidence of T2D was evaluated from the day of the baseline health examination with CT imaging to the day of the last health examination before 31 December 2018.

Assessment of Glycemic Traits and Aerobic Capacity in Germany

After an overnight fast, a 5-point 75-g oral glucose tolerance test was performed. We evaluated glycemia using the area under the curve (AUC) of glucose from 0 to 120 min (AUC $Glucose_{0–120}$). Insulin sensitivity was assessed with the nonesterified fatty acids–based insulin sensitivity index (NEFA-ISI), and insulin secretion was quantified by the ratio of the AUC of C-peptide from 0 to 30 min to the AUC of glucose from 0 to 30 min (AUC $C\text{-peptide}_{0–30}$/AUC $Glucose_{0–30}$) (34). To estimate insulin secretion adjusted for insulin sensitivity, we computed the residuals of AUC $C\text{-peptide}_{0–30}$/AUC $Glucose_{0–30}$ from a linear regression of this variable on NEFA-ISI and its quadratic term. Analytes were measured as described previously (23). We evaluated aerobic capacity (maximal oxygen uptake [Vo_{2max}]) on a bicycle ergometer as previously described (35).

Cluster Analysis

To identify fat distribution clusters in Japan, we used liver attenuation, pancreas attenuation, muscle attenuation, and visceral fat area. Liver attenuation, pancreas attenuation, and muscle attenuation were "flipped," such that higher values corresponded to more fat. To account for sex-related differences in fat distribution, we standardized each of the four indices (mean = 0, SD = 1) separately for the men and for the women in the randomly selected subcohort (n = 658). With these sex-stratified standardized variables, we conducted k-means clustering using the kmeans function in R. We selected a k value of 4 based on visual inspection of the elbow plot and majority vote of multiple indices to determine the best number of clusters using the NbClust function in R (36). We created a two-dimensional cluster plot based on principal components analysis using the fviz_cluster

function in R. Jaccard similarities to the original cluster with 2,000 resamplings were calculated to evaluate cluster stability with use of the cboot.hclust function in R. We named the clusters based on cluster variable means.

To assign each of the 754 Japanese participants to one of the clusters generated from the randomly selected subcohort, we used the cluster centroids to identify the cluster nearest to each participant by performing k-nearest neighbor classification with k = 1 using the knn function in R. We used the assigned clusters to evaluate the risk of T2D.

As a validation test of the fat distribution clusters, we applied the cluster analysis described above to 319 participants in the TDFS German cohort. We used the validated clusters to evaluate glycemic traits in the cohort in Germany.

Statistical Analysis

Baseline characteristics of the participants were compared between fat distribution clusters using Fisher exact test for categorical data and Wilcoxon rank sum tests or the Kruskal-Wallis test for continuous data.

Using the data from Japan, we conducted weighted Cox regression analyses to evaluate the association between the fat distribution clusters and the incidence of T2D. Besides unadjusted analysis and analyses adjusted for age and sex, we conducted three multivariable analyses. In model 1, we adjusted for age, sex, alcohol intake (daily alcohol intake or not), current smoking, and muscle area. In model 2, we further adjusted for BMI. In model 3, we further adjusted for systolic blood pressure, diastolic blood pressure, triglycerides, HDL cholesterol, LDL cholesterol, antihypertensive drugs, and lipid-lowering drugs. Despite a high correlation of BMI with visceral fat, we adjusted for BMI to investigate the importance of fat distribution clusters independent from BMI. We also quantified interactions among pairs of the four fat indices (liver attenuation, pancreas attenuation, muscle attenuation, and visceral fat area on CT) regarding the incidence of T2D.

Using the data from Germany, we estimated the mean and 95% CI of the AUC $\text{Glucose}_{0–120}$, NEFA-ISI, AUC $\text{C-peptide}_{0–30}$/AUC $\text{Glucose}_{0–30}$, and AUC $\text{C-peptide}_{0–30}$/AUC $\text{Glucose}_{0–30}$ residuals in the fat distribution clusters. We also compared these glycemic traits using Wilcoxon rank sum test. We also quantified interactions among pairs of the four fat indices (liver fat, pancreas fat, muscle fat, and visceral fat volume on MRI) regarding the AUC $\text{Glucose}_{0–120}$. In addition, linear regression models were used to evaluate the association of each fat index with NEFA-ISI, AUC $\text{C-peptide}_{0–30}$/AUC $\text{Glucose}_{0–30}$, AUC $\text{C-peptide}_{0–30}$/AUC $\text{Glucose}_{0–30}$ residuals, and Vo_{2max}.

For statistical analyses, R, version 4.0.5 (R Foundation for Statistical Computing, Vienna, Austria), and Stata 17 (StataCorp, College Station, TX) were used.

Ethics Considerations

The study in Japan was approved by the ethics committees of Kyoto University and Keijinkai Maruyama Clinic, and written informed consent was not required because it was retrospective. The study in Germany was approved by the ethics committee of the University of Tübingen, and written informed consent was provided by all participants before enrollment.

Data and Resource Availability

The data generated during the current study are not publicly available due to them containing information that could compromise research participant privacy/consent. No applicable resources were generated or analyzed during the current study.

RESULTS

Participants' Characteristics and k-Means Clustering

Table 1 shows baseline data. k-means clustering identified four similarly configured clusters in both Japan and Germany (Fig. 1 and Supplementary Fig. 3). Participants in cluster 1 had the highest levels of liver fat as well as somewhat high levels of visceral fat, so cluster 1 was called the hepatic steatosis cluster. Participants in cluster 2 had the highest levels of pancreas fat, as well as somewhat high levels of visceral fat and muscle fat, so cluster 2 was called the pancreatic steatosis cluster. Participants in cluster 3 had high levels of muscle fat, so cluster 3 was called the trunk myosteatosis cluster. Participants in cluster 4 had low levels of fat in all compartments, so cluster 4 was called the steatopenia cluster. Details of the clusters are shown in Supplementary Table 1 and Supplementary Table 2. The stability of each cluster was estimated as its Jaccard mean, which was $\geq$0.8 for all clusters except cluster 2 in Germany, for which it was 0.64.

Association Between Fat Distribution Clusters and Incidence of T2D

With the steatopenia cluster as the reference, hazard ratios (HRs) and 95% CIs for the association of the other three clusters with incidence of T2D are shown in Table 2. In the unadjusted analysis, HRs for T2D incidence in all three clusters were greater than the reference value of 1. After adjustment for age, sex, alcohol intake, current smoking, and muscle area, the associations of steatosis with T2D were still substantial for all three clusters. After further adjustment for BMI, the effect sizes were smaller, but the HRs for T2D incidence in both the hepatic steatosis cluster and the pancreatic steatosis cluster were still greater than the reference value of 1 ($P < 0.001$ and $P = 0.016$, respectively). Results of pairwise comparisons are shown in Supplementary Table 3.

Pairwise Interactions of Fat Compartments Regarding T2D Risk

Three interactions were found (Supplementary Table 4), and all three involved pancreas fat: visceral fat and pancreas fat (P for interaction = 0.004), liver fat and

Table 1—Baseline characteristics

	Japan			
	Noncase subjects (n = 608)	Case subjects (n = 146)	P	Germany, total (n = 319)
Age (years)	51 (43–59)	54 (47–59)	0.009	44 (34–60)
Male, n (%)	440 (72.4)	128 (87.7)	<0.001	87 (27.3%)
BMI (kg/m^2)	23.5 (21.6–25.8)	25.7 (23.6–28.7)	<0.001	27.0 (23.0–31.5)
CT-based indicators				
Liver fat (HU)	65.1 (60.4–68.4)	59.7 (49.4–65.2)	<0.001	N/A
Pancreas fat (HU)	48.8 (43.4–52.3)	44.6 (39.1–48.5)	<0.001	N/A
Muscle fat (HU)	40.8 (36.1–44.9)	39.3 (35.9–42.7)	0.009	N/A
Visceral fat (cm^2)	86.3 (37.7–142.5)	156.1 (109.6–206.0)	<0.001	N/A
Muscle area (cm^2)	142.8 (110.5–161.6)	158.2 (138.8–174.8)	<0.001	N/A
MRI-based indicators				
Liver fat (%)	N/A	N/A		2.2 (0.8–5.8)
Pancreas fat (%)	N/A	N/A		3.5 (1.9–6.3)
Muscle fat (%)	N/A	N/A		7.1 (5.8–8.6)
Visceral fat (L)	N/A	N/A		2.6 (1.5–4.4)
Muscle area (cm^2)	N/A	N/A		134.9 (123.1–158.7)
Fasting plasma glucose (mg/dL)	90.0 (84.0–95.0)	106.0 (97.0–113.0)	<0.001	91.8 (84.6–97.2)
Fasting plasma glucose (mmol/L)	5.0 (4.7–5.3)	5.9 (5.4–6.3)	<0.001	5.1 (4.7–5.4)
HbA_{1c} (%)	5.3 (5.1–5.4)	5.8 (5.5–6.0)	<0.001	5.5 (5.3–5.8)
HbA_{1c} (mmol/mol)	34 (32–36)	40 (37–42)	<0.001	37 (34–40)
Triglycerides (mg/dL)	92.0 (64.5–132.5)	122.5 (87.0–190.0)	<0.001	91.0 (65.0–123.0)
HDL cholesterol (mg/dL)	57.0 (48.0–67.0)	51.0 (44.0–59.0)	<0.001	54.0 (46.0–66.0)
LDL cholesterol (mg/dL)	120.0 (102.0–140.5)	130.0 (102.0–153.0)	0.025	115.0 (97.0–142.0)
Systolic blood pressure (mmHg)	120.0 (110.0–130.0)	125.0 (120.0–136.0)	<0.001	130.0 (118.0–141.0)
Diastolic blood pressure (mmHg)	76.0 (70.0–81.0)	80.0 (72.0–88.0)	<0.001	84.0 (77.0–92.0)
Current smoker, n (%)	176 (28.9)	53 (36.3)	0.089	22 (7.2)
Alcohol intake, n (%)	213 (35.0)	51 (34.9)	1.00	14 (4.6)
Family history of diabetes, n (%)	120 (19.7)	36 (24.7)	0.21	180 (56.4)
Antihypertensive drug, n (%)	82 (13.5)	47 (32.2)	<0.001	18 (5.6)
Lipid-lowering drug, n (%)	67 (11.0)	23 (15.8)	0.12	7 (2.2)

Continuous data are expressed as median (interquartile range). Fisher exact test and Wilcoxon rank sum tests were used to compare noncase subjects with case subjects in Japan. Missing data: muscle volume (n = 9), systolic blood pressure (n = 1), diastolic blood pressure (n = 1), current smoker (n = 14), alcohol intake (n = 13). N/A, not applicable.

pancreas fat (P for interaction = 0.055), and muscle fat and pancreas fat (P for interaction = 0.001).

Differences in Glycemic Traits Across Fat Distribution Clusters

With the steatopenia cluster as the reference, glycemic traits of the other three fat distribution clusters are shown in Table 3. Participants who were in the hepatic steatosis cluster had the highest glycemia ($P < 0.001$) and the lowest insulin sensitivity ($P < 0.001$). Compared with the participants in the steatopenia cluster, those in the pancreatic steatosis cluster had higher glycemia ($P < 0.001$), lower insulin sensitivity ($P < 0.001$), and the lowest insulin secretion with adjustment for insulin sensitivity ($P = 0.081$). Among those in the trunk myosteatosis cluster, glycemia was high ($P < 0.001$), insulin sensitivity was low ($P < 0.001$), and insulin secretion adjusted for insulin sensitivity was low ($P = 0.081$). Results of pairwise comparisons are shown in Supplementary Table 5.

Pairwise Interactions of Fat Compartments Regarding Glycemia

Five interactions were found (Supplementary Table 6). P values for all five interactions were <0.01. The only interaction term that was not significantly different from zero was the term for the interaction between liver fat and muscle fat (P for interaction = 0.34).

Association of Single Fat Compartments With Insulin and With Aerobic Capacity

All four fat compartments were associated with insulin sensitivity (Supplementary Table 7) ($P < 0.001$), with the largest effect size observed for visceral fat. Only pancreas fat was associated with lower insulin secretion adjusted

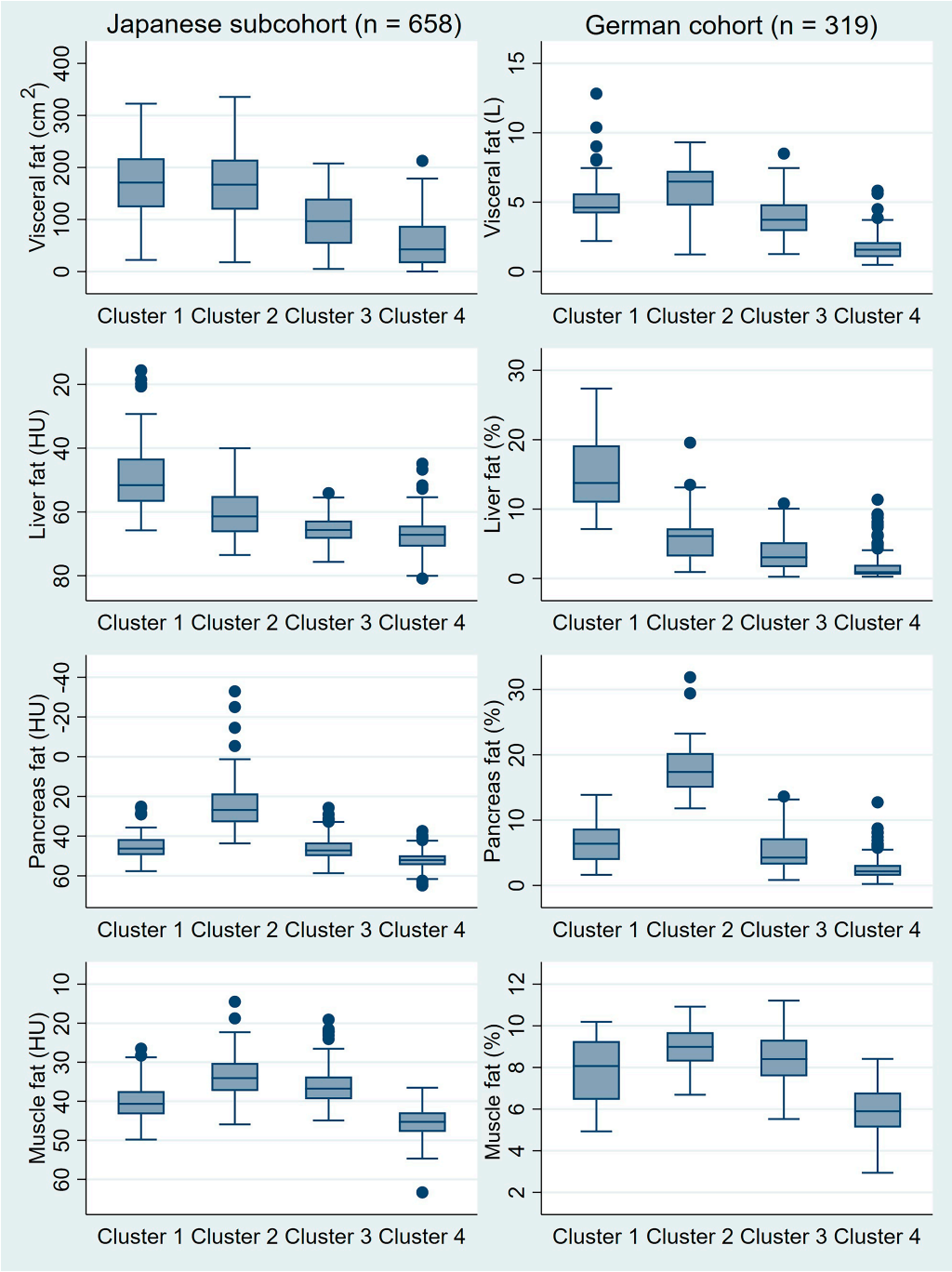

Figure 1—k-means clustering of fat distribution. Distributions of visceral fat, liver fat, pancreas fat, and muscle fat are shown. k-means clustering resulted in four clusters: a hepatic steatosis cluster (cluster 1), a pancreatic steatosis cluster (cluster 2), a trunk myosteatosis cluster (cluster 3), and a steatopenia cluster (cluster 4).

for insulin sensitivity ($P = 0.016$). All four fat compartments were associated with lower aerobic capacity, with the largest effect size observed for muscle fat.

DISCUSSION

Individuals without diabetes had a highly heterogenous distribution of fat in the liver, pancreas, skeletal muscle, and visceral areas. Independently applying data-driven partitioning procedures to two cohorts, we identified four patterns (four clusters) of fat distribution: a hepatic steatosis cluster, a pancreatic steatosis cluster, a trunk myosteatosis cluster, and a steatopenia cluster. An individual's risk of T2D was associated with a specific pattern of fat distribution. Compared with the individuals who had low levels of fat in all areas studied (i.e., those in the steatopenia

Table 2—HRs and 95% CIs for the association between grouping in a fat distribution cluster at baseline and incidence of diabetes, from the case-cohort study in Japan (n = 754)

	Cluster 1: hepatic steatosis	Cluster 2: pancreatic steatosis	Cluster 3: trunk myosteatosis	Cluster 4: steatopenia
Subcohort	118 (17.9)	62 (9.4)	224 (34.0)	254 (38.6)
Cases of type 2 diabetes*	56 (38.4)	23 (15.8)	44 (30.1)	23 (15.8)
Unadjusted analysis	5.49 (3.25–9.27), <0.001	5.15 (2.73–9.71), <0.001	2.36 (1.38–4.01), 0.002	1.00 (reference)
Age- and sex-adjusted analysis	5.15 (3.02–8.79), <0.001	3.74 (1.85–7.57), <0.001	1.98 (1.09–3.58), 0.024	1.00 (reference)
Multivariable-adjusted model 1	4.02 (2.27–7.12), <0.001	3.38 (1.65–6.91), 0.001	1.95 (1.07–3.54), 0.029	1.00 (reference)
Multivariable-adjusted model 2	3.23 (1.69–6.15), <0.001	2.65 (1.20–5.87), 0.016	1.76 (0.96–3.24), 0.068	1.00 (reference)
Multivariable-adjusted model 3	3.23 (1.62–6.44), 0.001	2.52 (1.12–5.67), 0.026	1.65 (0.88–3.10), 0.12	1.00 (reference)

Data are n (%) or HR (95% CI), P value. Weighted Cox regression analyses were conducted for estimation of the HRs, 95% CIs, and P values. Model 1: adjustment for age, sex, alcohol intake, current smoking, and muscle area. Model 2: adjustment for age, sex, alcohol intake, current smoking, muscle area, and BMI. Model 3: adjustment for age, sex, alcohol intake, current smoking, muscle area, BMI, systolic blood pressure, diastolic blood pressure, triglycerides, HDL cholesterol, LDL cholesterol, antihypertensive drugs, and lipid-lowering drugs. *Includes case subjects within and outside of the randomly selected subcohort.

cluster), those in the other three clusters were at a greater risk of incident T2D. The distribution of T2D risk among clusters in one cohort was similar to the distribution of glycemia among clusters in the other cohort. Insulin sensitivity and insulin secretion differed across clusters, which indicates the pathophysiologic contributions of each fat distribution pattern to T2D risk (Supplementary Fig. 4).

Our results are consistent with those of previous studies: individuals with a high amount of visceral fat and liver fat had a high risk of T2D. Both visceral fat at baseline and its increase over time were strongly linked to high incidence of T2D (3). In a meta-analysis, liver fat was found to be associated with a twofold higher risk of T2D (12). The underlying mechanism most likely involves hepatic and whole-body insulin resistance, by direct effects on hepatocytes and/or by effects on remote organs mediated by hepatokines (37,38). Our present study confirmed the well-established associations of visceral fat and liver fat with insulin resistance.

Two longitudinal studies detected associations of pancreas fat accumulation with increased risk of T2D (7,18). The underlying mechanism is thought to be unfavorable effects of this local fat accumulation on pancreatic insulin secretion (8,14). However, pancreas fat is not always detrimental for insulin secretion. In previous MRI and pathological studies, the association between pancreas fat and insulin secretion impairment was found in individuals

Table 3—Glycemia, insulin sensitivity, and insulin secretion based on results of 75-g oral glucose tolerance tests, across fat distribution clusters in Germany (n = 319)

	Cluster 1: hepatic steatosis (n = 39)	Cluster 2: pancreatic steatosis (n = 21)	Cluster 3: trunk myosteatosis (n = 103)	Cluster 4: steatopenia (n = 156)
Glycemia				
AUC $Glucose_{0–120}$	1,038.9 (969.4–1,108.4)	980.7 (905.1–1056.4)	956.5 (920.7–992.3)	806.7 (777.3–836.1)
P	<0.001	<0.001	<0.001	Reference
Insulin sensitivity				
NEFA-ISI	2.1 (1.9–2.3)	3.0 (2.3–3.8)	3.4 (3.1–3.6)	5.5 (5.2–5.8)
P	<0.001	<0.001	<0.001	Reference
Insulin secretion				
AUC C-$peptide_{0–30}$/AUC $Glucose_{0–30}$	215.8 (194.4–237.2)	169.2 (138.2–200.1)	170.3 (158.2–182.5)	145.7 (137.1–154.2)
P	<0.001	0.12	<0.001	Reference
Sensitivity-adjusted insulin secretion				
AUC C-$peptide_{0–30}$/AUC $Glucose_{0–30}$ residuals	9.7 (−9.1 to 28.5)	−15.2 (−37.2 to 6.8)	−5.9 (−16.8 to 5.1)	3.2 (−4.8 to 11.2)
P	0.57	0.081	0.081	Reference

Means and 95% CIs are shown. The unit of measure for AUC $Glucose_{0–120}$ is mmol * min/mL. Insulin sensitivity and secretion are in arbitrary units. P values were calculated from Wilcoxon rank sum tests comparing the steatopenia cluster with the other clusters. To estimate insulin secretion adjusted for insulin sensitivity, we calculated AUC C-$peptide_{0–30}$/AUC $Glucose_{0–30}$ residuals from the regression of AUC C-$peptide_{0–30}$/AUC $Glucose_{0–30}$ on NEFA-ISI and its quadratic term. Missing data: insulin sensitivity (n = 3), insulin secretion (n = 4), sensitivity-adjusted insulin secretion (n = 7).

with high genetic risk for diabetes but not in those with low genetic risk. Especially, the genetic risk related to insulin resistance and liver lipid metabolism modulated the relationship between pancreas fat and insulin secretion (17). All of these findings show how the effect of pancreas fat on T2D can be modified by many factors, including genetic risk, metabolic state, and other interacting fat compartments (7,8). Coculture models suggest the presence of a complex organ-organ cross talk modulating insulin secretion (16,39). k-means clustering revealed a fat distribution pattern that might fuel such a detrimental interorgan cross talk. Specifically, individuals in the pancreatic steatosis cluster had lower insulin secretion than expected for their degree of insulin resistance. The hypothesis that pancreatic fat exerts its detrimental effects in combination with other factors is further supported by interactions between fat in the pancreas and in the other tested compartments in terms of glycemia and diabetes risk.

One interesting finding of our current analysis is the contribution of muscle fat to the fat distribution patterns that are associated with T2D risk. The relations among muscle fat accumulation, insulin resistance, and T2D are complex (40). While findings of several cross-sectional analyses suggested that muscle fat can be a risk factor for insulin resistance and T2D (9,10,13), it is well-known that fat also accumulates in the muscle of athletes who are very insulin sensitive (13,40). Most prior studies evaluated muscle fat in the lower extremities, but here we quantified fat in trunk muscle (41). In concert with fat at other locations, fat in trunk muscle appears to link to T2D risk via muscle and systemic insulin resistance (13). In a few previous studies investigators have already looked at lower-extremity muscle fat when analyzing body fat distribution patterns and T2D. Miljkovic et al. (10) simultaneously evaluated liver fat, muscle fat, and visceral fat in nonobese individuals. They showed that liver fat and muscle fat were associated with concurrent T2D. Unlike in the current study, in that study *incident* T2D was not evaluated and pancreas fat was not measured. In another recent study (42), subgroups defined by fat accumulation were identified and were found to be associated with T2D, but that study was also cross-sectional and pancreas fat was not evaluated.

Besides comprehensively investigating multiple fat compartments that are known to affect T2D pathogenesis, we aimed to address organ-organ interplay with our clustering approach (16,39). This approach bore fruit, with the finding of interactions between fat compartments for glycemia and T2D risk. Furthermore, the clusters identified in this study had specific constellations of fat distribution and were strongly linked to T2D risk, likely via differences in insulin sensitivity and insulin secretion. Further studies are warranted to uncover the detailed mechanisms of interplay among fat in different locations.

One limitation of this study is the fact that the cohorts were not population based, so they might not reflect the general population. Moreover, we cannot exclude that fat accumulation in the analyzed trunk muscle behaves differently compared with other muscle compartments. Furthermore, there was some loss to follow-up, with a follow-up rate of 85% in Japan.

In conclusion, using information on patterns of fat distribution, we identified four distinct groups of individuals. Of note, the pattern of fat distribution was strongly associated with insulin sensitivity, with insulin secretion, and with the likelihood of future T2D. Unlike separately investigating fat in each location, this new approach provides information on the interplay of excess fat in different locations. Our findings underline the importance of body fat distribution rather than general adiposity. They can provide a basis for more individualized approaches to preventing and treating T2D.

Acknowledgments. The authors thank Keita Numata from the System Development Section, Keijinkai Maruyama Clinic, and Kunihiko Hayashi, Hiromitsu Yonezawa, Eiji Kazuta, Kimihiro Saito, Keiko Takasaki, and Miyuki Yoshioka from the Department of Radiology, Keijinkai Maruyama Clinic. For comments and suggestions on an earlier version of the manuscript, the authors acknowledge the assistance of Joseph Green (Graduate School of Medicine, University of Tokyo).

Funding. This work was funded in part by the German Center for Diabetes Research (DZD) (Federal Ministry of Education and Research in Germany, 01GI0925), by the state of Baden-Württemberg (32-5400/58/2, Forum Gesundheitsstandort Baden-Württemberg), and by Japan Society for the Promotion of Science KAKENHI grants JP19K16978 and JP22K15685.

Duality of Interest. R.W. reports lecture fees from Novo Nordisk and Sanofi. R.W. served on an advisory board for Akcea Therapeutics, Daiichi Sankyo, Sanofi, and Novo Nordisk. M.H. reports research grants from Boehringer Ingelheim and Sanofi (both to the University Hospital Tübingen) and lecture fees from Amryt, Novo Nordisk, and Boehringer Ingelheim. He also served on an advisory board for Boehringer Ingelheim. No other potential conflicts of interest relevant to this article were reported.

Author Contributions. H.Y., R.W., and M.H. designed the study. S.T., J.M., T.H., M.D., N.H., and Y.K. collected data. H.Y., R.W., and M.H. wrote the draft of the manuscript. H.Y., J.M., T.H., and R.W. analyzed data. H.Y., S.T., J.M., T.H., Y.Y., M.D., N.H., Y.K., A.K., N.S., A.F., A.L.B., R.W., and M.H. reviewed the manuscript, made critical revisions, and approved the manuscript before submission. H.Y. (for the Japanese data) and R.W. and M.H. (for the German data) are the guarantors of this work and, as such, had full access to all the data in the study and take responsibility for the integrity of the data and the accuracy of the data analysis.

Prior Presentation. Parts of this study were presented in abstract form at the 82nd Scientific Sessions of the American Diabetes Association, New Orleans, LA, 3–7 June 2022.

References

1. Cefalu WT, Andersen DK, Arreaza-Rubín G, et al.; Symposium planning committee, moderators, and speakers. Heterogeneity of diabetes: β-cells, phenotypes, and precision medicine: proceedings of an international symposium of the Canadian Institutes of Health Research's Institute of Nutrition, Metabolism and Diabetes and the U.S. National Institutes of Health's National Institute of Diabetes and Digestive and Kidney Diseases. Diabetes Care 2022;45:3–22

2. Stefan N. Causes, consequences, and treatment of metabolically unhealthy fat distribution. Lancet Diabetes Endocrinol 2020;8:616–627

3. Wander PL, Boyko EJ, Leonetti DL, McNeely MJ, Kahn SE, Fujimoto WY. Change in visceral adiposity independently predicts a greater risk of developing

type 2 diabetes over 10 years in Japanese Americans. Diabetes Care 2013; 36:289–293
4. Yamazaki H, Tsuboya T, Tsuji K, Dohke M, Maguchi H. Independent association between improvement of nonalcoholic fatty liver disease and reduced incidence of type 2 diabetes. Diabetes Care 2015;38:1673–1679
5. Yamazaki H, Wang J, Tauchi S, et al. Inverse association between fatty liver at baseline ultrasonography and remission of type 2 diabetes over a 2-year follow-up period. Clin Gastroenterol Hepatol 2021;19:556–564.e5
6. Martin S, Sorokin EP, Thomas EL, et al. Estimating the effect of liver and pancreas volume and fat content on risk of diabetes: a Mendelian randomization study. Diabetes Care 2022;45:460–468
7. Yamazaki H, Tauchi S, Wang J, et al. Longitudinal association of fatty pancreas with the incidence of type-2 diabetes in lean individuals: a 6-year computed tomography-based cohort study. J Gastroenterol 2020;55:712–721
8. Wagner R, Eckstein SS, Yamazaki H, et al. Metabolic implications of pancreatic fat accumulation. Nat Rev Endocrinol 2022;18:43–54
9. Correa-de-Araujo R, Addison O, Miljkovic I, et al. Myosteatosis in the context of skeletal muscle function deficit: an interdisciplinary workshop at the National Institute on Aging. Front Physiol 2020;11:963
10. Miljkovic I, Kuipers AL, Cvejkus RK, et al. Hepatic and skeletal muscle adiposity are associated with diabetes independent of visceral adiposity in nonobese African-Caribbean men. Metab Syndr Relat Disord 2020;18:275–283
11. Neeland IJ, Poirier P, Després JP. Cardiovascular and metabolic heterogeneity of obesity: clinical challenges and implications for management. Circulation 2018; 137:1391–1406
12. Mantovani A, Byrne CD, Bonora E, Targher G. Nonalcoholic fatty liver disease and risk of incident type 2 diabetes: a meta-analysis. Diabetes Care 2018;41:372–382
13. Petersen MC, Shulman GI. Mechanisms of insulin action and insulin resistance. Physiol Rev 2018;98:2133–2223
14. Petrov MS, Taylor R. Intra-pancreatic fat deposition: bringing hidden fat to the fore. Nat Rev Gastroenterol Hepatol 2022;19:153–168
15. Brøns C, Grunnet LG. Mechanisms in endocrinology: skeletal muscle lipotoxicity in insulin resistance and type 2 diabetes: a causal mechanism or an innocent bystander? Eur J Endocrinol 2017;176:R67–R78
16. Gerst F, Wagner R, Kaiser G, et al. Metabolic crosstalk between fatty pancreas and fatty liver: effects on local inflammation and insulin secretion. Diabetologia 2017;60:2240–2251
17. Wagner R, Jaghutriz BA, Gerst F, et al. Pancreatic steatosis associates with impaired insulin secretion in genetically predisposed individuals. J Clin Endocrinol Metab 2020;105:3518–3525
18. Chan TT, Tse YK, Lui RN, et al. Fatty pancreas is independently associated with subsequent diabetes mellitus development: a 10-year prospective cohort study. Clin Gastroenterol Hepatol. 25 September 2021 [Epub ahead of print]. DOI: 10.1016/j.cgh.2021.09.027
19. Barlow WE, Ichikawa L, Rosner D, Izumi S. Analysis of case-cohort designs. J Clin Epidemiol 1999;52:1165–1172
20. Breslow NE, Lumley T, Ballantyne CM, Chambless LE, Kulich M. Using the whole cohort in the analysis of case-cohort data. Am J Epidemiol 2009; 169:1398–1405
21. Yamashita Y, Murayama S, Okada M, et al. The essence of the Japan Radiological Society/Japanese College of Radiology imaging guideline. Jpn J Radiol 2016;34:43–79
22. Kulathinal S, Karvanen J, Saarela O, Kuulasmaa K. Case-cohort design in practice - experiences from the MORGAM Project. Epidemiol Perspect Innov 2007;4:15
23. Babbar R, Heni M, Peter A, et al. Prediction of glucose tolerance without an oral glucose tolerance test. Front Endocrinol (Lausanne) 2018;9:82
24. Kodama Y, Ng CS, Wu TT, et al. Comparison of CT methods for determining the fat content of the liver. AJR Am J Roentgenol 2007;188:1307–1312
25. Kim SY, Kim H, Cho JY, et al. Quantitative assessment of pancreatic fat by using unenhanced CT: pathologic correlation and clinical implications. Radiology 2014;271:104–112
26. Schweitzer L, Geisler C, Pourhassan M, et al. What is the best reference site for a single MRI slice to assess whole-body skeletal muscle and adipose tissue volumes in healthy adults? Am J Clin Nutr 2015;102:58–65
27. Cespedes Feliciano EM, Popuri K, Cobzas D, et al. Evaluation of automated computed tomography segmentation to assess body composition and mortality associations in cancer patients. J Cachexia Sarcopenia Muscle 2020;11:1258–1269
28. Faron A, Sprinkart AM, Kuetting DLR, et al. Body composition analysis using CT and MRI: intra-individual intermodal comparison of muscle mass and myosteatosis. Sci Rep 2020;10:11765
29. Goodpaster BH, Kelley DE, Thaete FL, He J, Ross R. Skeletal muscle attenuation determined by computed tomography is associated with skeletal muscle lipid content. J Appl Physiol (1985) 2000;89:104–110
30. Machann J, Thamer C, Stefan N, et al. Follow-up whole-body assessment of adipose tissue compartments during a lifestyle intervention in a large cohort at increased risk for type 2 diabetes. Radiology 2010;257:353–363
31. Würslin C, Machann J, Rempp H, Claussen C, Yang B, Schick F. Topography mapping of whole body adipose tissue using A fully automated and standardized procedure. J Magn Reson Imaging 2010;31:430–439
32. Machann J, Hasenbalg M, Dienes J, et al. Short-term variability of proton density fat fraction in pancreas and liver assessed by multiecho chemical-shift encoding-based MRI at 3 T. J Magn Reson Imaging. 27 January 2022 [Epub ahead of print]. DOI: 10.1002/jmri.28084
33. Isensee F, Jaeger PF, Kohl SAA, Petersen J, Maier-Hein KH. nnU-Net: a self-configuring method for deep learning-based biomedical image segmentation. Nat Methods 2021;18:203–211
34. Hudak S, Huber P, Lamprinou A, et al. Reproducibility and discrimination of different indices of insulin sensitivity and insulin secretion. PLoS One 2021; 16:e0258476
35. Hoffmann C, Schneeweiss P, Randrianarisoa E, et al. Response of mitochondrial respiration in adipose tissue and muscle to 8 weeks of endurance exercise in obese subjects. J Clin Endocrinol Metab 2020;105:e4023–e4037
36. Charrad M, Ghazzali N, Boiteau V, Niknafs A. NbClust: an R package for determining the relevant number of clusters in a data set. J Stat Softw 2014;61:1–36
37. Meex RCR, Watt MJ. Hepatokines: linking nonalcoholic fatty liver disease and insulin resistance. Nat Rev Endocrinol 2017;13:509–520
38. Stefan N, Cusi K. A global view of the interplay between non-alcoholic fatty liver disease and diabetes. Lancet Diabetes Endocrinol 2022;10:284–296
39. Gerst F, Wagner R, Oquendo MB, et al. What role do fat cells play in pancreatic tissue? Mol Metab 2019;25:1–10
40. Gilbert M. Role of skeletal muscle lipids in the pathogenesis of insulin resistance of obesity and type 2 diabetes. J Diabetes Investig 2021;12:1934–1941
41. Maltais A, Alméras N, Lemieux I, et al. Trunk muscle quality assessed by computed tomography: association with adiposity indices and glucose tolerance in men. Metabolism 2018;85:205–212
42. Linge J, Whitcher B, Borga M, Dahlqvist Leinhard O. Sub-phenotyping metabolic disorders using body composition: an individualized, nonparametric approach utilizing large data sets. Obesity (Silver Spring) 2019;27:1190–1199